The molecular basis of vancomycin resistance in clinically relevant *Enterococci:* Crystal structure of D-alanyl-D-lactate ligase (VanA)

David I. Roper*†, Trevor Huyton†, Alexei Vagin, and Guy Dodson

York Structural Biology Laboratory, Department of Chemistry, The University of York, Heslington, York YO10 5DD, United Kingdom

Edited by Christopher T. Walsh, Harvard Medical School, Boston, MA, and approved May 17, 2000 (received for review March 16, 2000)

D-alanine-D-lactate ligase from *Enterococcus faecium* BM4147 is directly responsible for the biosynthesis of alternate cell-wall precursors in bacteria, which are resistant to the glycopeptide antibiotic vancomycin. The crystal structure has been determined with data extending to 2.5-Å resolution. This structure shows that the active site has unexpected interactions and is distinct from previous models for D-alanyl-D-lactate ligase mechanistic studies. It appears that the preference of the enzyme for lactate as a ligand over D-alanine could be mediated by electrostatic effects and/or a hydrogen-bonding network, which principally involve His-244. The structure of D-alanyl-D-lactate ligase provides a revised interpretation of the molecular events that lead to vancomycin resistance.

x-ray crystal structure

Resistance to commonly used antibiotics is a major clinical problem. The treatment of life-threatening Gram-positive infections, such as those caused by methicillin-resistant *Staphylococcus aureus* (MRSA), for example, depends at present on treatment with antibiotics such as vancomycin and teicoplanin. Vancomycin is now the last line of defense against MRSA and many other multiple-antibiotic-resistant infections. It targets the peptidoglycan cell wall of Gram-positive bacteria by selectively binding the D-alanine-D-alanine (D-Ala) termini of peptidoglycan precursors and preventing their cross linking to adjacent strands. This significantly weakens the structural integrity of the cell wall and leads to osmotic lysis. Recently, however, strains of *Streptococcus pneumoniae*, the most common cause of sepsis and meningitis, have become tolerant to vancomycin (1). Because the more common high-level forms of vancomycin resistance are associated with five genes encoded by mobile genetic elements (2), there is a real probability that this resistance mechanism could well be acquired by other virulent life-threatening infectious agents such as MRSA. The clinical isolates resistant to vancomycin are characterized by a subtle change in the structure of peptidoglycan termini, as a result of the action of D-alanyl-D-X ligases, which have dual-subsite specificity at their second amino acid-binding site. The switch from D-Ala-D-Ala peptidoglycan termini to D-alanine-D-lactate (D-Ala-D-Lac) results in the loss of crucial hydrogen-bonding interactions, causing a 1,000-fold reduction of vancomycin-binding affinity.

Inducible high-level vancomycin resistance in *Enterococcus faecium* BM4147 is associated with the five genes located on the transposable element Tn1546 and is the most common clinical phenotype (2). A two-component transcriptional-activation system of VanS and VanR controls the induction of three structural genes VanH, VanA, and VanX. VanH is an α-keto acid reductase that converts pyruvate to D-Lac for D-Ala-D-Lac synthesis by the ATP-dependent desipeptide ligase, VanA (3). VanA is a 38.5-kDa protein capable of utilizing both hydroxyl acids and D-Ala as substrates with a concomitant switch from ester to peptide bond formation dependent on pH (4). The presence of any peptidoglycan chains ending in D-Ala-D-Ala, as a consequence of endogenous peptidoglycan biosynthesis genes, is negated by the action of VanX, a Zn^{2+}-dependent D-Ala-D-Ala dipeptidase (5). Thus the action of these three genes in concert ensures the production of D-Ala-D-Lac-terminating peptidoglycan chains, which are bound very weakly by the glycopeptide antibiotic vancomycin, rendering the bacteria resistant.

The first step in defining the structural and biochemical basis of vancomycin resistance was the determination of the structure of the enzyme [D-Ala-D-Ala ligase (DdlB), from *Escherichia coli*] that synthesizes the D-Ala-D-Ala moiety incorporated into the normal vancomycin-susceptible cell walls (6). The sequence of VanA and DdlB exhibits ≈40% identity, and their overall folds are very similar. The enzymes have similar functions in the biosynthesis of peptidoglycan termini in bacteria, but the capacity of VanA to form D-Ala-D-Lac has a direct correlation with enterococcal resistance to vancomycin. In this paper, we report the crystal structure of VanA complexed with a substrate inhibitor (7) and define the residues involved in substrate binding that are crucial to the resistance mechanism.

Materials and Methods

Purification and Crystallization. The purification and crystallization of the enzyme have been described in detail elsewhere (8). Briefly, the enzyme was crystallized by the hanging-drop-vapor diffusion method in the presence of a phosphinate inhibitor analogue of D-Ala-D-Ala between 40% and 45% ammonium sulfate, 0.1 M Mops, pH 6.0, with crystals reaching dimensions of $0.4 \times 0.2 \times 0.1$ mm. A native dataset to 2.5 Å resolution was collected and the space group determined as $C222_1$ with cell dimensions of a = 123.2 Å, b = 225 Å, and c = 72.4 Å, with a single dimer in the asymmetric unit. Data were collected with an oscillation range of 1° per image by using a Cu-K_a radiation source and a MAR345 image plate device. Crystals were soaked in mother liquor containing a glycerol concentration of 35% as cryoprotectant before flash vitrification in a stream of N_2 gas at 120 K. The data were processed and reduced by using the HKL suite of programs (9).

Structure Determination and Refinement. Numerous attempts to solve the structure of VanA by molecular replacement by using a variety of programs had proved unsuccessful until recent in-house developments in the molecular replacement program MOLREP (10) became available. A solution was obtained by using

This paper was submitted directly (Track II) to the PNAS office.

Abbreviations: D-Ala, D-alanine; D-Lac, D-lactate; DdlB, *E. coli* D-Ala-D-Ala ligase; VanA, *E. faecium* BM4147 D-Ala-D-Lac ligase.

Data deposition: The atomic coordinates have been deposited in the Protein Data Bank, www.rcsb.org (PDB ID code 1E4E).

*To whom reprint requests should be addressed. E-mail: roper@ysbl.york.ac.uk.

†D.I.R. and T.H. contributed equally to this work.

The publication costs of this article were defrayed in part by page charge payment. This article must therefore be hereby marked "*advertisement*" in accordance with 18 U.S.C. §1734 solely to indicate this fact.

Article published online before print: *Proc. Natl. Acad. Sci. USA*, 10.1073/pnas.150116497. Article and publication date are at www.pnas.org/cgi/doi/10.1073/pnas.150116497

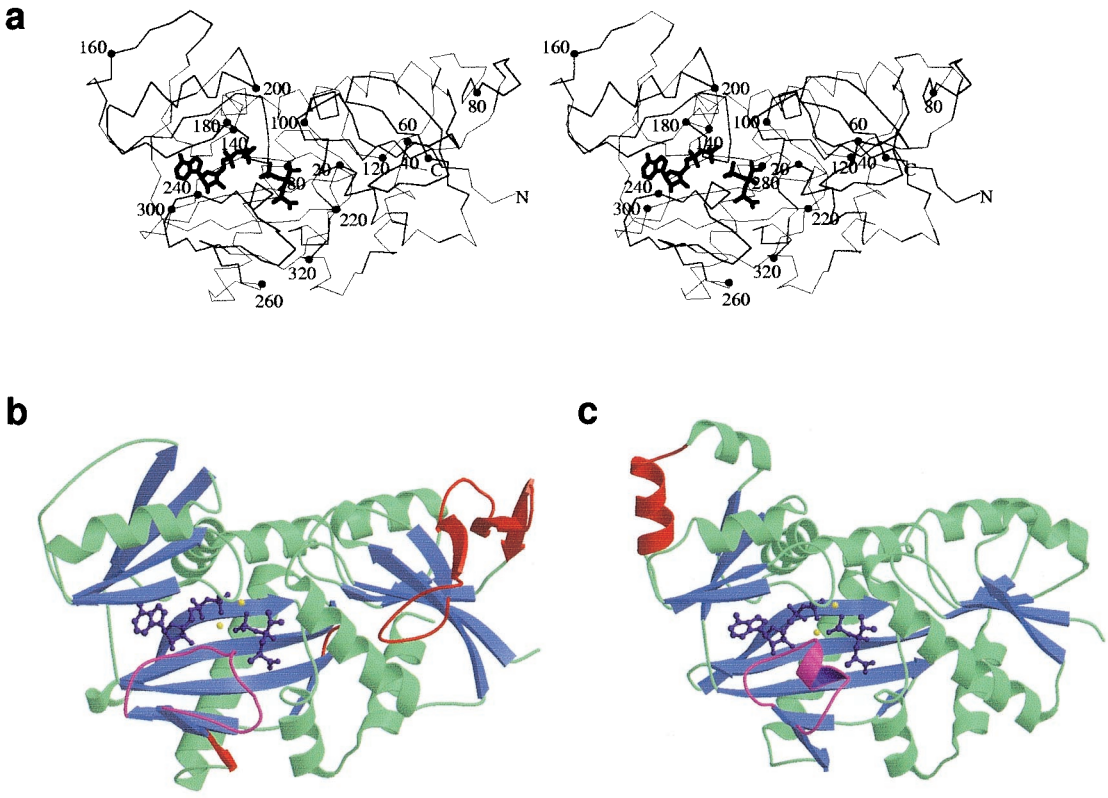

Fig. 1. Stereo C-α trace of VanA (*a*) with ADP and phosphophosphinate inhibitor showing overall structural features. Every twentieth residue is highlighted with a closed circle. N and C termini are marked N and C, respectively. In *b* and *c*, the structures of VanA and DdlB were overlaid in the program QUANTA and aligned by using close-residue optimization. Helices are displayed in green and β sheets in blue. ADP and phosphinophosphinate inhibitor are displayed in purple and magnesium ions in yellow. The ω-loops of both VanA and DdlB are displayed in magenta to highlight structural differences. Structural features corresponding to amino acid sequence found in one protein compared with the other are shown in red. In the structural alignment, a large additional loop occurs in VanA, between residues 44 and 90. The N terminus of each protein is shown on the right of each structure, immediately before the beginning of a β sheet found in both DdlB and VanA.

the structure of the DdlB Y216F mutant (PDB ID no. 1IOW) as a search model (11), enabling the position of the VanA dimer within the asymmetric unit to be determined. Before refinement, 5% of the data were randomly flagged for cross-validation analysis (12). Rigid-body refinement as implemented in the program REFMAC (13) was performed on a polyalanine model of the structure solution divided into three domains. Refinement was carried out starting from 6 Å resolution with gradual increments in resolution to 2.5 Å. Individual atomic parameters were refined by using REFMAC. With noncrystallographic restraints, R_{cryst} and R_{free} values were reduced to 46% and 50%, respectively. Initial phases were derived from these coordinates by the program CAD (14) and improved by averaging, solvent flattening, and histogram matching in the program DM (15), by using a figure of merit calculated in REFMAC. Rebuilding from this initial model was carried out by using the X-AUTOFIT routine implemented in the program QUANTA (Molecular Simulations, San Diego, CA). After several cycles of rebuilding and refinement, the density-modified maps were of sufficient quality to allow the modeling of residues 2–342, one ATP molecule and one phosphinate transition state inhibitor per molecule. In addition, a total of 397 waters, 3 sulfate ions, and 21 glycerol molecules were modeled and included in refinement. The electron density associated with the glycerol molecules was larger than that for a typical water and had a shape consistent with the branched structure of glycerol. In many cases, the density suggested that the glycerols were in more than one arrangement. Generally, the atoms refined with very high B-factors, similar to the mobile water molecules. It was decided at this stage not to try to interpret these complex peaks in more detail either as water or glycerol. The concentration of glycerol in the mother liquor was 35%. Final refinement converged to an R_{cryst} value of 0.205 and an R_{free} value of 0.284 for data in the range of 15–2.5 Å.

Results and Discussion

Structure of VanA in Complex with ADP and Phosphinate Inhibitor. The tertiary structure of VanA in complex with ADP and a phosphorylated phosphinate inhibitor, an analogue of the transition-state species (7), is shown in Fig. 1*a*. The crystal structure is well defined, with the electron-density maps continuous from residues 2 to 342, the penultimate residue at the C terminus. The structure has been refined with data extending to 2.5 Å; statistical data for the final model are presented in Table 1. The side-chain density for the two terminal residues is insufficient to model side-chain atoms accurately, and these terminal residues have been assigned as alanine in our model. The enzyme's structure can be divided into three domains with the nucleotide- and substrate-binding sites formed predominantly between the central and C-terminal domains; it has the characteristics of the ATP-dependent carboxylate–amine/thiol ligase superfamily (16–19). The N-terminal domain runs from Ala-2 to Gly-121 and has an α/β structure containing two α-helices and eight β-strands. A loop extending from the ends of two of these strands supports Glu-16, which is involved in substrate binding at the first subsite and two residues, Val-19 and His-99, which are involved in stabilizing the carboxyl anion of the transition-state intermediate seen in the structure. Additionally, in the N-terminal domain there is unambiguous density for a disulphide bridge

Table 1. X-ray structure statistics for VanA

Data collection (parentheses refer to highest resolution bin)	
Resolution	15 Å–2.5 Å (2.54–2.50 Å)
Number of independent reflections	32,814
Completeness	93.3% (96.6%)
R_{merge}	5.8% (21.7%)
I/σI	29.9% (4.1%)
Refinement (parentheses refer to ideal values)	
Reflections used in refinement	31,150
Reflections used in R_{free}	1,664
R_{free}	28.4%
R_{cryst}	20.5%
RMS deviation from ideality:	
Bond lengths	0.012 Å (0.02 Å)
Bond angles	0.039° (0.04°)
Overall average B-factor	44.8
Average B-factor (ADP)	40.7
Average B-factor (phospinate inhibitor)	38.5
Average B-factor (waters)	54.4

formed between cysteines 52 and 64, which is not present in DdlB. This disulphide bond was unexpected; VanA is a bacterial intracellular enzyme and therefore is normally in a reducing environment. However, the positioning of this disulphide bridge is interesting in that it links two adjacent β-strands at the base of a short loop. It is likely that formation of this disulphide bond may have aided in the crystallization of VanA, as this disulphide-stabilized loop makes some crystal contacts to other molecules within the crystallographic unit cell (8). The central domain runs from residues Cys-122 to Ser-211 and is composed of three α-helices and four β-strands, whereas the C-terminal domain (Gly-212 to Ala-342) is composed of three α-helices and five β-strands. The majority of the residues involved in substrate and nucleotide binding are present at the interface between these two domains.

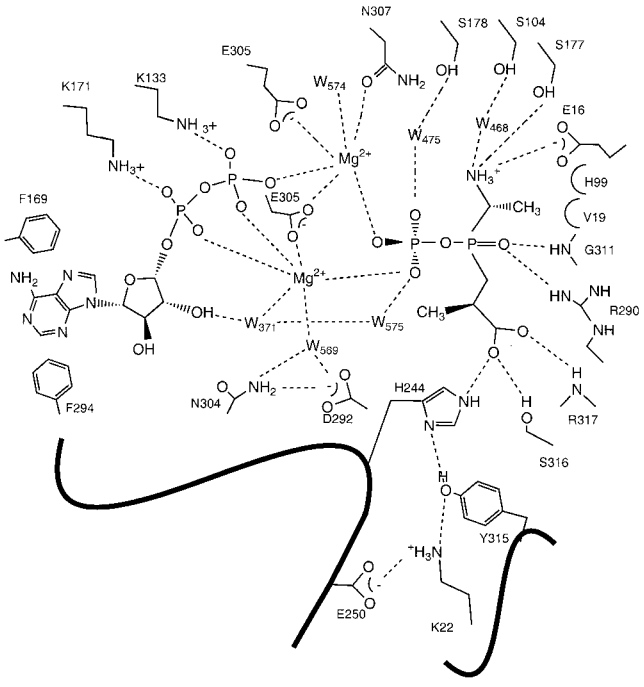

Fig. 2. Schematic diagram of the active site of VanA from the structure showing the interaction of various water molecules in addition to amino acid side chains. The protein backbone of the residues in the region of His-244 and Tyr-315 is shown as a solid black line. Hydrogen bond distances between Tyr-315, His-244, and the second subsite carboxyl oxygen of the transition state inhibitor are 2.77 Å and 2.74 Å, respectively. Two phenylalanine residues (F169 and F294) form stacking interactions with the adenine nucleotide rings. Several water molecules in the active site form interactions with the phosphate and magnesium atoms as well as amino acid side chains. There is an additional hydrogen bond between water 475 and water 371, which is not shown for clarity.

Comparison of VanA with DdlB. Analysis of the amino acid residues in close proximity to the substrate analogue shows there is a high degree of conservation between the two structures, except in the ω-loop region, which defines the active-site residues in DdlB (4, 6, 20, 21). The reactions of VanA and DdlB are similar in that both have two steps: first the initial D-Ala substrate is bound and phosphorylated, and second, the peptide or acyl bond is formed by the second substrate (D-Ala or D-Lac) in a nucleophilic reaction. Moreover, it has been pointed out (22) that D-Ala in the free-base state is, to a first approximation, an equally good substrate in VanA and DdlB. The distinctive property of VanA is therefore its capacity to select D-Lac preferentially at physiological pH.

An extra 37 residues are found in VanA compared with DdlB. Inspection of the overlaid structures by using QUANTA (Molecular Simulations) clearly shows the presence of a number of extended loops in the VanA N-terminal domain that account for the majority of these extra amino acids (see Fig. 1 *b* and *c*). However, these additional loops have no obvious function in relation to the altered substrate activity of the enzyme. Detailed comparison reveals that the ω-loop region, which is important in activity, differs in structure and composition between the two enzymes. In DdlB, this segment consists of residues 205–220 and contains two residues, Lys-215 and Tyr-216, within a short two-turn helix (H9) (6). These residues provide crucial hydrogen bonds to the β-phosphate oxygen atoms of ADP and maintain a hydrogen bond triad with Glu-15 and Ser-150. In VanA, the equivalent region (Arg-242–Asn-255) exists simply as an extended loop. Inspection of this loop in VanA reveals that His-244 replaces Tyr-216 and presents the appropriate chemistry for the switch from peptide to catalytically assisted ester bond-forming activity on binding D-lactate (see Fig. 2).

A more detailed comparison of the active sites of DdlB and VanA identifies a conserved water molecule, 444, in the second subsite (not shown). It makes four tetrahedral hydrogen bonds: with the side-chain amine of Arg-290 (Arg-255 in DdlB), with the main-chain nitrogen of Tyr-318 (Val-282 in DdlB), with the main-chain carbonyl of Gly-311 (Gly-276 in DdlB), and with the carboxylate group of the inhibitor in the second subsite. However, consideration of its position and hydrogen-bonding interactions make it an unlikely candidate to participate in the abstraction of a proton from the incoming nucleophile during catalysis (see below); presumably this water has a structural role.

A second and unanticipated feature of the VanA loop is the replacement of the DdlB Lys-215, which interacts directly with and balances the charge of the phosphate group by a network of four well-ordered waters (475, 371, 569, and 575) (see Fig. 3 *a* and *b*). These waters form a stabilizing hydrogen bond network to the oxygens of both phosphates of ADP, to one of the bound magnesium atoms, and to the phosphate of the transition-state analogue. This arrangement of water molecules also displaces Asn-292 (Asn-257 in DdlB), which now coordinates to its nearest magnesium atom via water molecule 569, also bound by Asn-304. The second magnesium atom in the VanA active site maintains the interactions with the ADP and inhibitor phosphates seen in DdlB and specifically hydrogen bonds with Glu-305 and Asn-307. These interactions are augmented by a bound water atom, 574 (not found in DdlB), and this in turn forms a network with the main-chain carbonyl on Ser-175 and adjacent water.

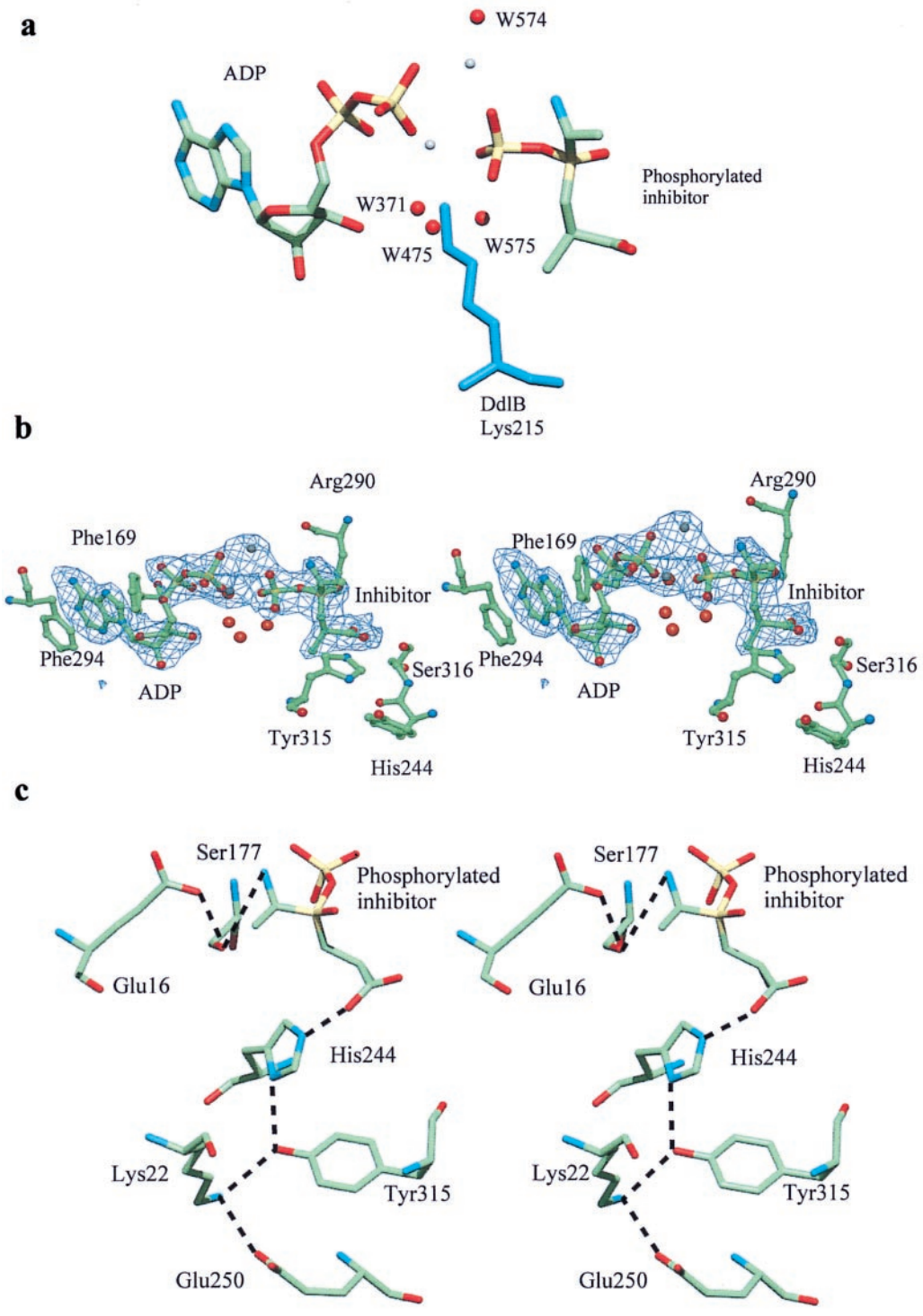

Fig. 3. (*a*) Comparison of active site waters in *E. facieum* VanA, which replace Lys-215 in *E. coli* DdlB. Magnesium atoms are shown in gray with water molecules in red. The structures of VanA and DdlB were superimposed and the relative positions of waters in VanA and Lys-215 in DdlB compared. Water 475 in VanA takes an equivalent position to the side-chain nitrogen of Lys-215 in DdlB. Hydrogen-bonding distances between adjacent water molecules, magnesium atoms, and phosphate atoms are not shown for clarity. Other water molecules, notably W371, W569, and W574, coordinate with magnesium ions in the active site of VanA. (*b*) A stereo representation and 2 $F_o - F_c$ map showing the active-site residues in contact with the phosphinophosphinate transition state intermediate. The map is contoured at 1σ by using the final 2.5-Å resolution map. Residues in the immediate vicinity of the transition state intermediate are marked. The two magnesium ions that coordinate with the phosphate ion of the intermediate and the β-phosphate of ADP are displayed in gray, and water molecules in this vicinity are displayed in red. Water 475 in VanA takes an equivalent position to the side-chain nitrogen of Lys-215 in DdlB. Other water molecules, notably W371 and W574, coordinate with magnesium ions in the active site of VanA. (*c*) Stereo diagram of the hydrogen bonding interacts with and in the vicinity of the phosphorylated phosphinate inhibitor in the active site. The Glu-250, Lys-22, Tyr-4315, and His-244 hydrogen-bonding network is shown, making a 2.7-Å hydrogen bond with the carboxylate oxygen of the inhibitor. This carboxylate also hydrogen bonds to a conserved serine (316 in VanA), which is not shown for clarity. The position of His-244 in our structure is such that it cannot make hydrogen-bonding interactions with the Glu-16 and Ser-177, which are structurally conserved in comparison to DdlB. The later two amino acids form important interactions that anchor D-Ala in the first subsite, an analogous situation to that found in DdlB.

A third difference between the two enzymes is the pattern of contacts with the ligand at the second subsite. This ligand has a phosphoryl group at the junction of the carbonyl amide bond and is a transition-state analogue. In the VanA complex, His-244 is in hydrogen-bonding distance to the inhibitor carboxylate: in DdlB, however, its spatial equivalent in DdlB, Tyr-216, makes no contacts to the inhibitor but is linked by hydrogen bonds to Ser-150 and Glu-15. It is assumed that the real substrate experiences these or similar interactions during binding and reaction. There will be differences, probably small, resulting from the absence of amide NH and ester O and the β-carbon. The hydrogen-bonding network equivalent to Tyr-216, Ser-150, and Glu-15 in DdlB is broken in the VanA inhibitor complex by the conformation of the imidazole ring in His-244 (see Fig. 3*c*). Nonetheless, in VanA the equivalent Ser-177 remains H-bonded to Glu-16. It is important to the discussion below on the VanA specificity that we expect, in the absence of substrate, that the His-244 forms a H-bonding pattern equivalent to that of Tyr-216 in DdlB.

The possible role of His-244 in the mechanism has been recently explored by site-directed mutagenesis (22). As discussed above, when VanA has only the phosphorylated alanine in its first subsite, His-244 is likely to be in a different position than that seen in the crystal structure complex, thus allowing access to the active site by the second ligand. Then a possible component in VanA's selectivity for lactate could come from the positive charge at His-244, which at neutral pH would at least be partly protonated, a state that would repel the alanine zwitter ion. And of course a positive charge on the His-244 would attract the negatively charged lactate to the second subsite. We note that the mutation His-244→Ala increases K_m by 77-fold (0.69 mM to 53 mM) for the D-lac substrate in the second site, producing a 170-fold change in the k_{cat}/K_m specificity constant (22). In contrast, the same mutation in VanA reduces the K_m for alanine by only 2-fold (160 mM to 87 mM), with a very slight increase in turnover. These observations demonstrate that the imidazole ring is important mainly in substrate specificity by preferentially favoring lactate binding over alanine. It is not obvious why this is so. The H-bonding to the carboxylate present in the inhibitor complex will occur presumably with D-Lac and D-Ala. There is no obvious interaction between His-244 and the phosphoryl oxygen and the inhibitor. Perhaps in the real substrate there is such an interaction, explaining the high K_m for D-Lac.

The kinetic data show that at pH 7.5, the k_{cat} for lactate is 35 per minute, and that of alanine, 500 (22), indicating that the enzyme's active site actually prefers the alanine as the second substrate. The mutational data (His-244→Ala) on VanA (22) indicate that the His-244 makes no significant contribution to k_{cat} for the alanine substrate; there is, on the other hand, a 2-fold reduction in k_{cat} with this mutation for lactate (22). Thus, although slower, the lactate reaction appears to involve His-244, possibly as a base. Because the pK of imidazole nitrogen is about pH 7, at neutral pH, a population of the His will be unprotonated and able to act as a base, potentially accepting protons from the lactate OH but evidently not from the alanine NH_2. In conclusion, therefore, VanA's heightened selectivity for lactate in comparison to other D-Ala-D-Lac ligases rests on the presence of His-244 as either a charged or neutral species and on the interactions it makes in the Michaelis complex. Supporting the structural role of His-244 in VanA is the structure of the D-Ala D-Lac ligase from *Leuconostoc mesenteroides*, a soil organism with intrinsic vancomycin resistance (23). In this enzyme, Phe-261 occupies the same spatial position as Tyr-216 in DdlB and His-244 in VanA. The recent x-ray structure for this enzyme suggests that the smaller size and greater hydrophobicity of the active site in comparison to DdlB contributes to selectivity for lactate over alanine (24). However, the *L. mesenteroides* enzyme has 10-fold lower selectivity than VanA, suggesting that the potential electrostatic interactions possible with histidine provide greater specificity.

On the basis of the structure of VanA detailed in this work, it would seem likely that the structure of VanB, an isofunctional enzyme from *Enterococcus faecalis* V583 (25) that also possesses D-Ala-D-Lac-forming activity, will be very similar to VanA. The two sequences are some 75% identical and, importantly, share very close sequence conservation in the VanA ω-loop; identical residues are found in the His-244 hydrogen-bond network. The situation with VanC and VanC2, which are D-Ala-D-serine ligase from *Enterococcus gallinarium* BM4174 and *Enterococcus flavescens*, respectively (26, 27), is less clear, however. Although there is obvious general sequence similarity between VanA, VanB, and the VanC subtypes, this does not include the all-important ω-loop region, where there appears to be a deletion in the VanC type sequences. A full explanation of these differences must await a structure determination from this family of enzymes. Further research into the structure and reactions of these and other related enzymes will help in the design of specific inhibitors and provide a route for new and effective antibiotic strategies.

We thank the following members of the Structural Biology Laboratory for help, advice, and support during this study: Drs. G. Davies, A. Pike, A. M. Brzozowski, J. Turkenburk, A. Cameron, R. Lewis, G. Murshudov, A. English, and E. J. Dodson. We also thank Professors Jim Knox for useful discussions and C. Walsh for providing information contained in refs. 22 and 24 before publication. D.I.R. is a Medical Research Council Career Development Fellow. The Structural Biology Laboratory is supported by the Biotechnology and Biological Sciences Research Council.

1. Novak, R., Henriques, B., Charpentier, E., Normark, S. & Tuomanen, E. (1999) *Nature (London)* **399,** 580–593.
2. Walsh, C. T., Fisher, S. L. Park, I.-S, Prahalad, M. & Wu, Z. (1996) *Chem. Biol.* **3,** 21–28.
3. Bugg, T. D. H., Wright, G., Dutka-Malen, S., Arthur, M., Courvalin, P. & Walsh, C. T. (1991) *Biochemistry* **30,** 10408–10415.
4. Park, I.-S., Lin, C.-H. & Walsh, C. T. (1996) *Biochemistry* **35,** 10464–10471.
5. Reynolds, P. E., Depardieu, F. , Dutka-Malen, S., Arthur, M. & Courvalin, P. (1994) *Mol. Microbiol.* **13,** 1065–1070.
6. Fan, C., Moews, P. C., Walsh, C. T. & Knox, J. R. (1995) *Science* **266,** 439–443.
7. Ellsworth, B. A. Tom, N. J. & Bartlett, P. A. (1996) *Chem. Biol.* **3,** 37–44.
8. Huyton, T. & Roper, D. I. (1999) *Acta Crystallogr. D* **55,** 1481–1483.
9. Otwinowski, Z. & Minor, W. (1997) *Methods Enzymol.* **276,** 307–326.
10. Vagin, A. A. & Teplyakov, A. (1997) *J. Appl. Crystallogr.* **30,** 1022–1025.
11. Fan, C., Park, I.-S., Walsh, C. T. & Knox, J. R. (1997) *Biochemistry* **36,** 2531–2538.
12. Brunger, A. T. (1992) *Nature (London)* **355,** 472–475.
13. Murshudov, G. N., Vagin, A. A. & Dodson, E. J. (1997) *Acta Crystallogr. D* **53,** 240–255.
14. Collaborative Computing Project No. 4 (1994) *Acta Crystallogr. D* **53,** 240–255.
15. Cowtan, K. & Main, P. (1998) *Acta Crystallogr. D* **54,** 487–493.
16. Fan, C., Moews, P. C., Shi, P. C., Walsh, C. T. & Knox, J. R. (1995) *Proc. Natl. Acad. Sci. USA* **92,** 1172–1176.
17. Artymiuk, P. J., Poirrett, A. R., Rice, D. W. & Willett, P. (1996) *Nat. Struct. Biol* **3,** 128–132.
18. Kobayashi, N. & Go, N. (1997) *Nat. Struct. Biol* **4,** 6–7.
19. Galperin, M. Y. & Koonin, E. V. (1997) *Protein Sci.* **6,** 2639–2643.
20. Shi, Y. & Walsh, C. T. (1995) *Biochemistry* **34,** 2768–2776.
21. Fan, C., Park, I.-S., Walsh, C. T. & Knox, J. R. (1997) *Biochemistry* **36,** 2531–2538.
22. Lessard, I. A. D., Healy, V. L., Park, I.-S. & Walsh, C. T. (1999) *Biochemistry* **38,** 14006–14022.
23. Park, I.-S. & Walsh, C. T. (1997) *J. Biol. Chem.* **272,** 9210–9214.
24. Kuzin, A. P., Sun, T., Jorczak-Baillass, J., Healy, V. L. Walsh, C. T. & Knox, J. R. (2000) *Structure (London)* **8,** 463–470.
25. Evers, S. & Courvalin, P. (1996) *J. Bacteriol.* **178,** 1302–1309.
26. Dutka-Malen, S., Molinas, C., Arthur, M. & Courvalin, P. (1992) *Gene* **112,** 53–58.
27. Park, I.-L., Lin, C.-H. & Walsh, C. T. (1997) *Proc. Natl. Acad. Sci. USA* **94,** 10040–10044.